ACS central science

Research Article

Cite This: ACS Cent. Sci. 2018, 4, 1194−1200

http://pubs.acs.org/journal/acscii

Visualizing Structural Transformation and Guest Binding in a Flexible Metal−Organic Framework under High Pressure and Room Temperature

Hui Yang,[†,‡] Feng Guo,[‡,§] Prem Lama,[∥] Wen-Yang Gao,[#] Hui Wu,[⊥] Leonard J. Barbour,*[,∥] Wei Zhou,*[,⊥] Jian Zhang,*[,†] Briana Aguila,[‡] and Shengqian Ma*[,‡]

[†]State Key Laboratory of Structural Chemistry, Fujian Institute of Research on the Structure of Matter, Chinese Academy of Sciences, Fuzhou 350002, P. R. China

[‡]Department of Chemistry, University of South Florida, 4202 East Fowler Avenue, Tampa, Florida 33620, United States

[§]School of Chemistry and Chemical Engineering, Yangtze Normal University, Chongqing 408100, P. R. China

[∥]Department of Chemistry and Polymer Science, University of Stellenbosch, Matieland 7602, South Africa

[⊥]NIST Center for Neutron Research, National Institute of Standards and Technology, Gaithersburg, Maryland 20899-6102, United States

[#]Department of Chemistry, Texas A&M University, College Station, Texas 77843, United States

Supporting Information

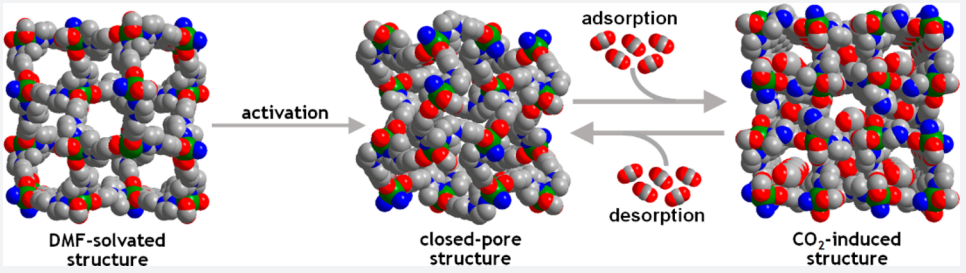

ABSTRACT: Understanding the effect of gas molecules on the framework structures upon gas sorption in porous materials is highly desirable for the development of gas storage and separation technologies. However, this remains challenging for flexible metal−organic frameworks (MOFs) which feature "gate-opening/gate-closing" or "breathing" sorption behaviors under external stimuli. Herein, we report such a flexible Cd-MOF that exhibits "gating effect" upon CO_2 sorption. The ability of the desolvated flexible Cd-MOF to retain crystal singularity under high pressure enables the direct visualization of the reversible closed-/open-pore states before and after the structural transformation as induced by CO_2 adsorption/desorption through *in situ* single-crystal X-ray diffraction experiments. The binding sites of CO_2 molecules within the flexible MOF under high pressure and room temperature have also been identified via combined *in situ* single-crystal X-ray diffraction and powder X-ray diffraction studies, facilitating the elucidation of the states observed during gate-opening/gate-closing behaviors. Our work therefore lays a foundation to understand the high-pressure gas sorption within flexible MOFs at ambient temperature, which will help to improve the design efforts of new flexible MOFs for applications in responsive gas sorption and separation.

INTRODUCTION

Metal−organic frameworks (MOFs), as an emerging type of crystalline porous material, have been of escalating interest due to their potential in a broad range of applications.[1] One of the striking features for MOFs in comparison with conventional porous materials, such as zeolites[2] and activated carbons,[3] lies in their structural flexibility/dynamics, as observed from the "gate-opening/gate-closing" or "breathing" sorption behaviors under external stimuli (e.g., adding or removing guest molecules, pressure, temperature).[4−7] Such flexible/dynamic MOFs hold particular promise for applications in selective gas adsorption,[8−13] gas storage,[14−19] and sensing.[20]

It is believed that the observed "gate-opening/gate-closing" or "breathing" sorption behaviors are associated with the structural transformations and the interplay between the host framework and the guest molecules during the adsorption/desorption processes.[19,21−28] It is of fundamental importance to understand the structural transformations and identify the interactions between the gas molecules and the host framework in these flexible/dynamic MOFs, which have been sought after using various techniques.[29−39] Given the difficulty in maintaining crystal singularity for desolvated flexible/dynamic

Received: June 18, 2018
Published: August 20, 2018

DOI: 10.1021/acscentsci.8b00378
ACS Cent. Sci. 2018, 4, 1194−1200

MOFs under high pressures and ambient temperatures, the studies to monitor their structural transformations have exclusively relied on *in situ* powder crystal X-ray diffraction (PXRD) tools, which however cannot provide unequivocal structural information as *in situ* single-crystal X-ray diffraction (SCXRD) experiments can.[19,35,36] This makes it even more challenging to crystallographically identify the binding sites of gas molecules within flexible/dynamic MOFs, which thus far are elucidated mainly through computational studies.[8,13,14,16,25]

In this contribution, we report a flexible three-dimensional (3D) microporous cadmium(II) MOF (Cd-MOF) with 4-fold interpenetration and diamondoid (dia) topology, which after desolvation shows an interesting "gating effect" process and "breathing" behavior upon CO_2 sorption. In addition, this flexible Cd-MOF can retain its crystal singularity in the absence of guest solvent molecules under high pressure, which therefore allows us, for the first time, to directly visualize the reversible closed/open end states of the structures induced by gas molecules for a flexible MOF through *in situ* SCXRD experiments. The elucidated structural information in combination with *in situ* PXRD facilitates the production of a clear map for the binding of guest gas molecules within a flexible MOF under high pressure and at room temperature.

RESULTS AND DISCUSSION

Crystallographic Visualization of Structural Transformation in Flexible Cd-MOF. The flexible Cd-MOF (hereafter denoted **1a**) was synthesized via a previously reported route with a slight modification.[40] Single-crystal X-ray diffraction analysis reveals that **1a** crystallizes in the tetragonal space group $P42_12$. In the structure of **1a**, each Cd(II) site displays distorted octahedral geometry, with coordination bonds to four oxygen and two nitrogen atoms from four different 4-(1*H*-2-methylimidazol-1-yl)benzoic acid (miba) ligands (Figure 1a, Figure S1). Each μ_2-miba ligand bonds to two adjacent Cd(II) centers via two carboxylate O atoms and one imidazolyl N atom (Figure 1a, Figure S1). The dihedral angle formed by the benzoate plane and the imidazole plane of miba is 56.4° (Figure 1a, Figure S3). The planarity of the ligand, as quantified by the N (imidazole)-phenyl centroid-C (carboxylate) angle, is 154° (Figure 1a, Figure S2). The Cd···Cd distance is 12.46 Å. Cd(II) metal centers are connected by the miba ligands to form a neutral three-dimensional (3D) framework with larger hexagonal and small rhombic 1D channels along the crystallographic *c* axis (Figure 1c, Figure S4). Each channel is occupied by structurally disordered solvent DMF molecules. The total solvent-accessible volume for **1a** is estimated to be 37.8% using the PLATON program.[41] The framework topology is identified as a 4-connected net with 4-fold interpenetration and symbol (dia) by considering each Cd site as the 4-connected node (Figure S5). The experimental PXRD of **1a** matches that of the calculated one from single-crystal data (Figure 2).

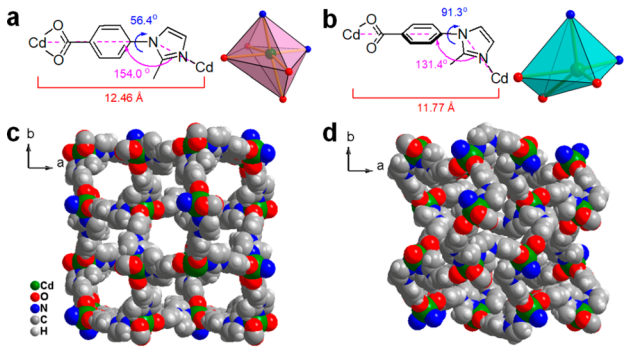

Figure 1. Cd···Cd distances, bond angles, and dihedral angles of the miba ligand and the coordination environment of the Cd(II) atoms of (a) **1a** and (b) **1b**. (c) Perspective along the *c* axis view of the 3D framework of **1a** showing 1D channels. (d) Perspective view along the *c* axis of the 3D structure of **1b**.

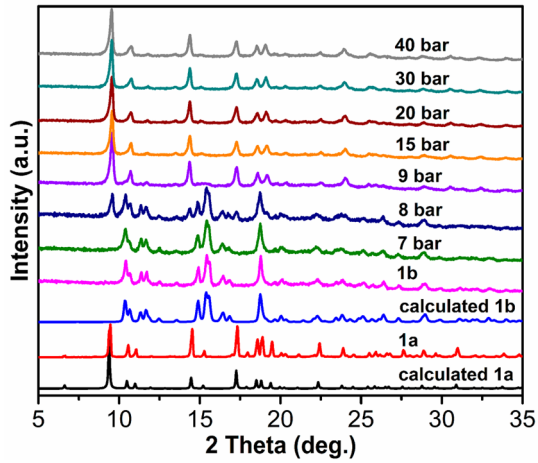

Figure 2. Comparison of the PXRD patterns of **1a** and **1b**, and the experimental patterns were recorded for the sample incrementally exposed *in situ* up to 40 bar CO_2 pressure.

To examine the possible structural transformation of the Cd-MOF, **1a** was activated by soaking freshly prepared crystals in dry dichloromethane to exchange guest DMF molecules followed by degassing under dynamic vacuum. The desolvated sample, named **1b** hereafter, still retained crystal singularity, allowing for SCXRD studies. The crystal data of **1a** and **1b** are summarized in Table S1. SCXRD analysis demonstrates that **1a** experiences drastic structural transformation upon desolvation to a dense (or closed) phase for **1b**. **1b** crystallizes in the orthorhombic space group $P2_12_12$ with a smaller (pseudotetragonal) unit cell and much lower solvent-accessible void volume (4.4%). The framework of **1b** undergoes changes in the coordination geometry of Cd(II), from six-coordinated octahedral geometry to five-coordinated hexahedral geometry (Figure 1b, Figure S6). During the transformation from **1a** to **1b** the Cd···Cd distance decreases significantly from 12.46 to 11.77 Å. The dihedral angle between the benzoate and imidazole planes increases from 56.4° to 91.3°, and the planarity of the ligand, as quantified by the N (imidazole)-phenyl centroid-C (carboxylate), decreases from 154° to 131.4° (Figure 1b, Figures S7 and S8). Moreover, the 1D channel becomes closed in **1b** as a result of "breathing effect" contortions (Figure 1d, Figure S9).[6,12,15,18,21,24,26,37] This observation is also supported by the PXRD data (Figure 2). Compared to **1a**, all of the characteristic peaks of **1b** in the PXRD pattern are shifted toward higher 2θ angles, and match well with the calculated ones (calculated from the crystallographic information file for **1b** with PXRD lattice parameters, see details in the Supporting Information, Figure 2).

To further probe the structural transformation from the open form **1a** to the closed form **1b**, we performed a detailed computational first-principles dispersion-corrected density-

DOI: 10.1021/acscentsci.8b00378
ACS Cent. Sci. 2018, 4, 1194−1200

functional theory (DFT-D) investigation (see details in the Experimental Section). The structures of **1a** and **1b** were first fully optimized. Then, nudged elastic band calculations were performed to find the minimum energy path of the structural transition. An animation consisting of structure snapshots along the minimal energy path shows clearly how the flexible framework evolves from a fully open-pore phase to a nearly closed-pore phase (see the movie in the Supporting Information). As expected, the imidazole and phenyl rings of the miba ligand remain relatively rigid. However, the bond connecting the two rigid rings and those coordinating the ligand to the Cd center are rather flexible, particularly in terms of bond angles. Such flexibility enables both the metal center and the organic linker to undergo a large degree of rotation and distortion upon crystal desolvation, leading to a configuration with dense framework packing, diminished pore volume, and low system energy.

CO_2 Sorption and *in Situ* Crystallographic Visualization of Structural Transformation under High Pressure. Capitalizing on the single-crystal to single-crystal "breathing effect" of **1a** and **1b**, we carried out CO_2 sorption experiments to assess the "gating effect" performance. A low-pressure CO_2 sorption isotherm was first measured at 195 K for a single sample of **1b**. The isotherm shows a broad gate-opening step with an onset pressure of ca. 0.34 bar, followed by a gradual increase in uptake at higher relative pressure (0.34 bar < P < 0.95 bar), indicating that a structural transformation occurs (Figure 3a). Upon desorption, a pronounced hysteresis

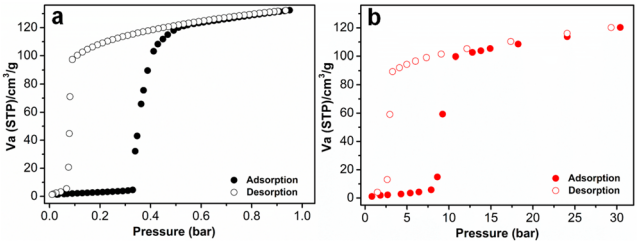

Figure 3. (a) CO_2 adsorption and desorption isotherms for **1b** at 195 K. (b) High-pressure CO_2 adsorption and desorption isotherms for **1b** at 298 K.

loop is observed at intermediate pressures (0.5−0.08 bar); a sudden decrease implies that a gate-closing phase transition occurs. The maximum uptake of CO_2 under the conditions used is 130 $cm^3\ g^{-1}$, which is equivalent to 6 CO_2 molecules per unit cell of **1b_open**.

Encouraged by the above CO_2 sorption results, we conducted high-pressure CO_2 sorption experiments on **1b** to evaluate the effect of the CO_2-induced framework structural transformation at 298 K in the pressure range 0−30 bar. The isotherm of **1b** exhibits very low uptake at the beginning (below 8 bar), followed by a steep increase at approximately 8 bar, which indicates a gate-opening transition (Figure 3b). An adsorption capacity commensurate with that at low temperature was reached upon saturation at approximately 30 bar. The total uptake (excess adsorption capacity) is 117 $cm^3\ g^{-1}$ (equivalent to a total adsorption capacity of 122 $cm^3\ g^{-1}$, 5.6 CO_2 molecules per unit cell of **1b_open**) at 30 bar. A sudden decrease at 3 bar on desorption indicates reversible switching between the open and closed phases. Variable-pressure *in situ* PXRD diffraction patterns (Figure 2, Figure S19) were recorded with incremental CO_2 loading to further investigate the gate-opening and gate-closing events at 298 K. The closed-pore phase of **1b** was confirmed under vacuum (Figure S19). Upon increasing the pressure, the closed-pore form for **1b** is still retained below 8 bar. Significant changes become apparent at 9 bar; the peaks of the closed phase diminish as peaks of the fully open phase appear, which indicates the structural transformation (gate-opening). As expected, this process of gate-opening and gate-closing, as monitored by PXRD, is in agreement with the CO_2 sorption results (Figure 3b, Figure S19). The open structure is retained over the pressure range 9−40 bar. Upon evacuation of the sample, the phase transforms (gate-closing) back to the closed-pore form for **1b** when the gas pressure is reduced to 2 bar or lower (Figure S20).

If these transformations can occur in single-crystal to single-crystal fashion, it would enable the characterization of each phase transition in a manner that is highly desired for flexible MOFs, which unfortunately tend to be poorly crystalline following breathing or swelling thereby limiting the collection of single-crystal data.[19,23] Fortunately, **1b** can maintain its single-crystal character even under high CO_2 pressure, which makes it possible for the first time to visualize the states before and after the structural transformation of a flexible MOF under high pressure through *in situ* SCXRD studies. Considering that unequivocal structural information for the high-pressure-induced open form of a flexible MOF has never been achieved, *in situ* SCXRD experiments were conducted on **1b** at the selected pressures of 15 and 20 bar, at which **1b** should feature the open-pore structure based on high-pressure CO_2 sorption isotherms (Figure 3b) and variable-pressure *in situ* PXRD diffraction patterns (Figure 2). Single-crystal structure analysis of **1b** under 15 bar CO_2 atmosphere (hereafter **1b_15 bar**) reveals that the structure of **1b_15 bar** is similar to the DMF-solvated structure of **1a** (Figures 1c and 4). The planarity of

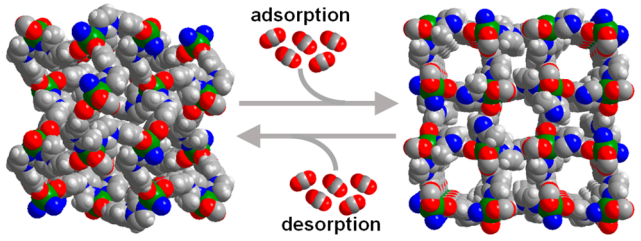

Figure 4. Reversible single-crystal to single-crystal transformation upon CO_2 adsorption/desorption: perspective view along the c axis, showing the closed-channel (left) and open-channel (right) of **1b_15 bar**. Note: the CO_2 guest molecules are diffuse (or disordered) in the 1D channels of **1b_15 bar**.

the miba ligand, as quantified by the N (pyridyl)-phenyl centroid-C (carboxylate) angle, is 154.5° in **1b_15 bar** close to 154.0° in **1a** (Figure 1a, Figures S11 and S18). The benzoate and imidazole planes exhibit dihedral angles of 53.2° and 56.4° for **1b_15 bar** and **1a**, respectively (Figure 1a, Figures S12 and S18). The Cd···Cd distances are almost the same in **1b_15 bar** (15.46 Å) and **1a** (15.45 Å) (Figure 1a, Figure S18). The opened rhombic and hexagonal channels are occupied by adsorbed CO_2 molecules, which are highly disordered and therefore not able to be well refined (Figure 4). Similar single-crystallographic data were determined for **1b** under 20 bar CO_2 atmosphere (the sample named **1b_20 bar**) (Table S1). The mechanism of structural flexibility of flexible MOFs such

DOI: 10.1021/acscentsci.8b00378
ACS Cent. Sci. 2018, 4, 1194−1200

as MIL-53,[6,24] MIL-88,[23] YO-MOF,[25] and RPM3-Zn[8] is mainly based upon hinge motion associated with carboxylate-ligands coordination. The SCXRD structural characterization of the various phases of **1b** clearly indicates that the transformation here largely relies upon the metal center and organic linker contortion. Moreover, **1b** might be stabilized by the interactions between interpenetrated dia networks.[19] To our knowledge, the rotation and distortion of the metal center and organic linker during adsorption/desorption of CO_2 molecules within the MOF pores are rare.[4−7]

Identification of Carbon Dioxide Binding within the Framework under High Pressure. To understand the interactions involved for the high-pressure gas-induced structural transformation of the flexible MOF, it is essential to elucidate how the gas molecules occupy the MOF pores. While both *in situ* SCXRD and *in situ* PXRD show clearly how the framework of **1b** evolves to open the pore upon CO_2 adsorption under high pressure, we found it difficult to directly resolve the atomic coordinates of the adsorbed CO_2 guest molecules from the SCXRD data. Therefore, we turned to DFT-D calculations for clues.

We first optimized the open-pore structure **1b_open**. CO_2 molecules were then introduced into the MOF pore, followed by a full relaxation (on both CO_2 positions and orientations). From the calculations, three major CO_2 adsorption sites were identified. Guided by the calculated MOF/CO_2 structure model, we further attempted to refine the PXRD data. We expected that the MOF pores would be more fully occupied at high pressure, and that the CO_2 molecules are likely more ordered within the pore (and could hopefully be better modeled). Therefore, we focused on the PXRD data of **1b_40 bar** (Figure 2, Table S1), and carried out a Rietveld structural refinement. To our delight, the refinement converged satisfactorily, and a reasonable goodness of fit was achieved (Figure 5, Table S1). From the refinement, we obtained an experimental crystal structure of **1b_40 bar(R)**, with detailed information on the adsorbed CO_2. We note that, at room temperature, there is inevitably some disorder associated with the adsorbed CO_2 (in terms of both positions and orientations) which was not modeled in the refinement. The structure derived from PXRD is regarded as an "average" structure, which we believe is still of value to understand the CO_2−framework interaction.

In the refined structure, there exist three preferential CO_2 adsorption locations (sites I, II, and III), as also suggested by the DFT-D calculations. All three sites are partially occupied, which is an indication of CO_2 disorder to some extent. Figure 6 shows schematically the 1D channels of the framework filled with CO_2 molecules located at these three sites. As in the structure of **1a**, there are two different types of channels in the open-pore structure of **1b_40 bar(R)**. Sites I and II are located in the wider channel while site III is in the narrower channel. The total calculated occupancy of these three sites is 5.9 CO_2 molecules per unit cell, which is consistent with the experimental results (5.6 and 6 CO_2 molecules per unit cell at 298 and 195 K, respectively). The interactions between the CO_2 molecules and the framework miba ligands consist mainly of van der Waals interactions.

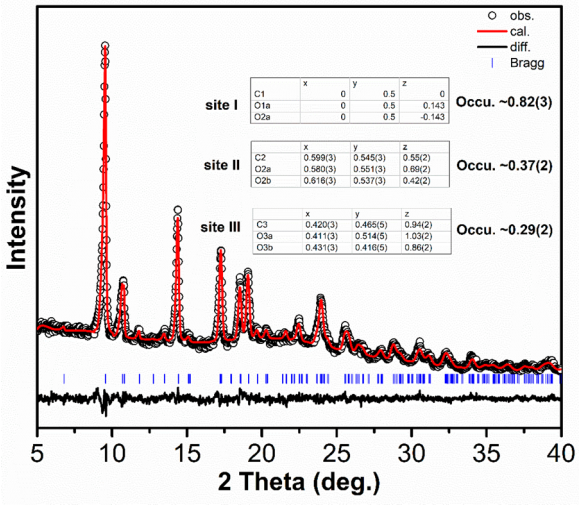

Figure 5. Rietveld refinement of the PXRD data of **1b_40 bar(R)**. Experimental (circles), calculated (line), and difference (line below observed and calculated patterns) powder diffraction profiles are shown. Vertical bars indicate the calculated positions of Bragg peaks. Goodness of fit data: R_p = 0.0382, R_{wp} = 0.0486.

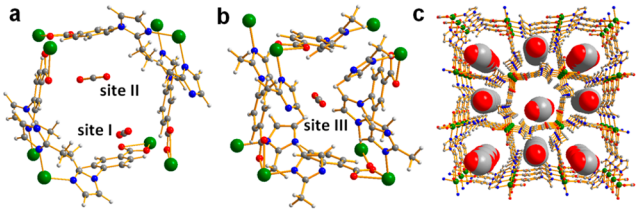

Figure 6. Crystal structure of **1b_40 bar(R)** from PXRD refinement showing (a, b) preferential binding sites for CO_2 uptake (sites I, II, and III), and (c) 3D framework of **1b_40 bar(R)** from PXRD refinement with guest CO_2 molecules in the channels.

Taken together, the above results demonstrate that the desolvated Cd-MOF exhibits extreme "breathing" behavior under high gas pressure at room temperature. Upon increasing/decreasing CO_2 pressure, the reversible closed-/open-pore states before and after the structural transformation have been directly visualized by *in situ* SCXRD techniques. The observed gate-opening/gate-closing can be ascribed to the rotation and distortion of the metal center and organic linker during adsorption/desorption of CO_2 molecules within the MOF pores. Rietveld structural refinements based on the DFT-D calculated structural model were carried out to gain an in-depth understanding of the CO_2−framework interaction. Three binding sites for CO_2 molecules with two in the larger hexagonal channel and one in the small rhombic 1D channel have been identified.

CONCLUSION

In summary, we reported a flexible 4-fold interpenetrated diamondoid Cd-MOF which displays unusual dynamic gating behavior upon CO_2 sorption. The open and closed states of a breathing framework as induced by CO_2 adsorption/desorption under high pressure and room temperature have been crystallographically observed through *in situ* SCXRD experiments. The interactions involved during the gate-opening/gate-closing have also been elucidated by identifying the binding sites of CO_2 molecules within the flexible MOF, thereby, the host−guest interactions via combined *in situ* SCXRD and PXRD studies. Our work therefore provides a clear map to understand the gas sorption within a flexible

DOI: 10.1021/acscentsci.8b00378
ACS Cent. Sci. 2018, 4, 1194−1200

MOF particularly at high pressure and ambient temperature, which will help to design new MOFs and other types of porous materials with pressure-induced gate-opening/gate-closing behaviors and lays the foundation for further understanding the mechanisms associated these processes for applications in task-specific gas sorption and separation.

EXPERIMENTAL SECTION

No unexpected or unusually high safety hazards were encountered.

Synthesis of 1a. **1a** was prepared using a reported procedure with a slight modification.[40] A mixture of Cd-$(NO_3)_2{\cdot}4H_2O$ (0.078 g), 4-(1*H*-2-methylimidazol-1-yl)-benzoic acid (Hmiba, 0.065 g), and DMF (6 mL) was sealed in a 23 mL polytetrafluoroethylene lined stainless steel container and heated to 85 °C for 3 days, and then cooled to room temperature. Colorless crystals of **1a** were obtained.

Preparation of 1b. A sample of **1a** was soaked in 20 mL of dry dichloromethane for 24 h. The solvent was replaced 6 times over 24 h, after which the sample was evacuated at 323 K for 300 min.

Characterization. Powder X-ray diffraction (PXRD) at ambient pressure was performed on a Rigaku X-ray diffractometer with a Cu Kα source. Pressure-resolved PXRD data were collected using Cu Kα radiation (λ= 1.5418 Å, 40 kV and 30 mA) on a PANalytical X'pert PRO instrument operating in Bragg−Brentano geometry. The sample was prepared in an environmental gas cell. CO_2 sorption data were collected at 195 K using automatic volumetric adsorption equipment, Micromeritics ASAP2020, after pretreatment under vacuum at 323 K for 300 min. High-pressure CO_2 sorption data were collected at 298 K. Thermogravimetric analyses (TGA) for all measurements were carried out on a PerkinElmer TGA thermogravimetric analyzer under air flow at a heating rate of 10 °C min^{-1} from 20 to 800 °C. Fourier transform infrared (FTIR) spectra were recorded on a ThermoElectron Nicolet high-resolution FT-MIR/FT-FarIR instrument in the range 4000−400 cm^{-1}.

Single-Crystal X-ray Diffraction. Single-crystal X-ray diffraction data for **1a**, **1b_15 bar**, and **1b_20 bar** were collected on a Bruker D8 Venture instrument equipped with a Photon II CPAD detector and an Oxford Cryosystems 800Plus cryostat, using graphite-monochromated Mo−Kα (λ = 0.710 73 Å) radiation. The single-crystal data of **1b** were obtained from a Bruker SMART APEX II CCD-based diffractometer with graphite-monochromatized Mo Kα radiation (λ = 0.710 73 Å).

For **1a**, the crystal was mounted on a glass fiber using super glue, and data were collected at room temperature. For **1b**, **1b_15 bar**, or **1b_20 bar** the crystal was mounted on a glass fiber inside an environmental gas cell.[35,42] Prior to data collection the gas cell was evacuated at ~2×10^{-3} mbar for 12 h to remove any potential traces of guest molecules or adsorbed water vapor. The crystal was then subjected to pressures of 15 bar (**1b_15 bar**) and 20 bar (**1b_20 bar**), and the data were collected for each of these pressures.

Data reduction was performed via a standard procedure with the use of the Bruker software package SAINT.[43] SADABS[44] was used for absorption corrections and correction of other systematic errors. The crystal structures were solved through direct methods utilizing SHELXS-97 and refined using SHELXL-97.[45] X-Seed[46] was employed as the graphical interface for the SHELX program suite. The contribution of disordered guest molecules was treated as diffuse with the utilization of the Squeeze procedure implemented in the Platon program.[41] All non-hydrogen atoms were refined anisotropically. Hydrogen atoms were placed in calculated positions using riding models.

Density-Functional Theory Calculations. First-principles density-functional theory calculations were performed using a Quantum-Espresso package.[47] A semiempirical addition of dispersive forces to conventional DFT (DFT-D) was included in the calculation to account for van der Waals interactions.[48] We used Vanderbilt-type ultrasoft pseudopotentials and the generalized gradient approximation (GGA) with the Perdew−Burke−Ernzerhof (PBE) exchange correlation. A cutoff energy of 544 eV and a 2 × 2 × 4 *k*-point mesh (generated using the Monkhorst−Pack scheme) were determined to be sufficient for total energy to converge within 0.01 meV $atom^{-1}$. To study the structural flexibility, full structural relaxations were first performed on **1a** and **1b** phases. Then, nudged elastic band calculations were performed to find the minimum energy path of the structural transition between **1a** and **1b**. To calculate the CO_2 adsorption sites, the open-pore structure of **1b_open** was optimized first. Then, CO_2 molecules were introduced to the optimized MOF structure, followed by full structural relaxations.

ASSOCIATED CONTENT

Supporting Information

The Supporting Information is available free of charge on the ACS Publications website at DOI: 10.1021/acscentsci.8b00378.

Crystal structures, TGA diagram, FTIR spectrum, *in situ* PXRD patterns, ^{1}H NMR spectra, and CCDC number and crystal data (PDF)

Flexible framework evolving from a fully open-pore phase to a nearly closed-pore phase (AVI)

Crystal structure of **1a** (CIF)

Crystal structure of **1b_15 bar** (CIF)

Crystal structure of **1b_20 bar** (CIF)

Crystal structure of **1b_40 bar(R)** (CIF)

Crystal structure of **1b** (CIF)

Crystal structure of **1b** with PXRD lattice parameters (CIF)

AUTHOR INFORMATION

Corresponding Authors

*E-mail: ljb@sun.ac.za.

*E-mail: wzhou@nist.gov.

*E-mail: zhj@fjirsm.ac.cn.

*E-mail: sqma@usf.edu.

ORCID

Hui Wu: 0000-0003-0296-5204

Leonard J. Barbour: 0000-0002-6453-8331

Wei Zhou: 0000-0002-5461-3617

Jian Zhang: 0000-0003-3373-9621

Shengqian Ma: 0000-0002-1897-7069

Notes

The authors declare no competing financial interest.

ACKNOWLEDGMENTS

We acknowledge financial support from NSFC (21425102 and 21521061), the Strategic Priority Research Program of the

DOI: 10.1021/acscentsci.8b00378
ACS Cent. Sci. 2018, 4, 1194−1200

Chinese Academy of Sciences (XDB20000000), the United States National Science Foundation (DMR-1352065), University of South Florida, and the National Research Foundation of South Africa. P.L. also acknowledges the Claude Leon Foundation for a postdoctoral fellowship.

REFERENCES

(1) Zhou, H. C.; Long, J. R.; Yaghi, O. M. Introduction to metal-organic frameworks. *Chem. Rev.* **2012**, *112*, 673−674.
(2) Li, Y.; Yu, J. New stories of zeolite structures: their descriptions, determinations, predictions, and evaluations. *Chem. Rev.* **2014**, *114*, 7268−7316.
(3) Xing, W.; Liu, C.; Zhou, Z.; Zhang, L.; Zhou, J.; Zhuo, S.; Yan, Z.; Gao, H.; Wang, G.; Qiao, S. Z. Superior CO_2 uptake of N-doped activated carbon through hydrogen-bonding interaction. *Energy Environ. Sci.* **2012**, *5*, 7323−7327.
(4) Horike, S.; Shimomura, S.; Kitagawa, S. Soft porous crystals. *Nat. Chem.* **2009**, *1*, 695−704.
(5) Schneemann, A.; Bon, V.; Schwedler, I.; Senkovska, I.; Kaskel, S.; Fischer, R. A. Flexible metal-organic frameworks. *Chem. Soc. Rev.* **2014**, *43*, 6062−6096.
(6) Ferey, G.; Serre, C. Large breathing effects in three-dimensional porous hybrid matter: facts, analyses, rules and consequences. *Chem. Soc. Rev.* **2009**, *38*, 1380−1399.
(7) Chang, Z.; Yang, D. H.; Xu, J.; Hu, T. L.; Bu, X. H. Flexible Metal-Organic Frameworks: Recent Advances and Potential Applications. *Adv. Mater.* **2015**, *27*, 5432−5441.
(8) Nijem, N.; Wu, H.; Canepa, P.; Marti, A.; Balkus, K. J.; Thonhauser, T.; Li, J.; Chabal, Y. J. Tuning the Gate Opening Pressure of Metal−Organic Frameworks (MOFs) for the Selective Separation of Hydrocarbons. *J. Am. Chem. Soc.* **2012**, *134*, 15201−15204.
(9) Carrington, E. J.; McAnally, C. A.; Fletcher, A. J.; Thompson, S. P.; Warren, M.; Brammer, L. Solvent-switchable continuous-breathing behaviour in a diamondoid metal−organic framework and its influence on CO_2 versus CH_4 selectivity. *Nat. Chem.* **2017**, *9*, 882−889.
(10) Couck, S.; Denayer, J. F.; Baron, G. V.; Remy, T.; Gascon, J.; Kapteijn, F. An amine-functionalized MIL-53 metal-organic framework with large separation power for CO_2 and CH_4. *J. Am. Chem. Soc.* **2009**, *131*, 6326−6327.
(11) Henke, S.; Schneemann, A.; Wutscher, A.; Fischer, R. A. Directing the breathing behavior of pillared-layered metal-organic frameworks via a systematic library of functionalized linkers bearing flexible substituents. *J. Am. Chem. Soc.* **2012**, *134*, 9464−9474.
(12) Llewellyn, P. L.; Bourrelly, S.; Serre, C.; Filinchuk, Y.; Férey, G. How Hydration Drastically Improves Adsorption Selectivity for CO_2 over CH_4 in the Flexible Chromium Terephthalate MIL-53. *Angew. Chem., Int. Ed.* **2006**, *45*, 7751−7754.
(13) Foo, M. L.; Matsuda, R.; Hijikata, Y.; Krishna, R.; Sato, H.; Horike, S.; Hori, A.; Duan, J.; Sato, Y.; Kubota, Y.; Takata, M.; Kitagawa, S. An Adsorbate Discriminatory Gate Effect in a Flexible Porous Coordination Polymer for Selective Adsorption of CO_2 over C_2H_2. *J. Am. Chem. Soc.* **2016**, *138*, 3022−3030.
(14) Lama, P.; Aggarwal, H.; Bezuidenhout, C. X.; Barbour, L. J. Giant Hysteretic Sorption of CO_2: In Situ Crystallographic Visualization of Guest Binding within a Breathing Framework at 298 K. *Angew. Chem., Int. Ed.* **2016**, *55*, 13271−13275.
(15) Jiang, Z.-Q.; Jiang, G.-Y.; Wang, F.; Zhao, Z.; Zhang, J. Controlling State of Breathing of Two Isoreticular Microporous Metal−Organic Frameworks with Triazole Homologues. *Chem. - Eur. J.* **2012**, *18*, 10525−10529.
(16) Mason, J. A.; Oktawiec, J.; Taylor, M. K.; Hudson, M. R.; Rodriguez, J.; Bachman, J. E.; Gonzalez, M. I.; Cervellino, A.; Guagliardi, A.; Brown, C. M.; Llewellyn, P. L.; Masciocchi, N.; Long, J. R. Methane storage in flexible metal−organic frameworks with intrinsic thermal management. *Nature* **2015**, *527*, 357−361.
(17) Llewellyn, P. L.; Horcajada, P.; Maurin, G.; Devic, T.; Rosenbach, N.; Bourrelly, S.; Serre, C.; Vincent, D.; Loera-Serna, S.; Filinchuk, Y.; Ferey, G. Complex adsorption of short linear alkanes in the flexible metal-organic-framework MIL-53(Fe). *J. Am. Chem. Soc.* **2009**, *131*, 13002−13008.
(18) Trung, T. K.; Trens, P.; Tanchoux, N.; Bourrelly, S.; Llewellyn, P. L.; Loera-Serna, S.; Serre, C.; Loiseau, T.; Fajula, F.; Férey, G. Hydrocarbon Adsorption in the Flexible Metal Organic Frameworks MIL-53(Al, Cr). *J. Am. Chem. Soc.* **2008**, *130*, 16926−16932.
(19) Yang, Q. Y.; Lama, P.; Sen, S.; Lusi, M.; Chen, K. J.; Gao, W. Y.; Shivanna, M.; Pham, T.; Hosono, N.; Kusaka, S.; Perry, J. J. t.; Ma, S.; Space, B.; Barbour, L. J.; Kitagawa, S.; Zaworotko, M. J. Reversible Switching between Highly Porous and Nonporous Phases of an Interpenetrated Diamondoid Coordination Network That Exhibits Gate-Opening at Methane Storage Pressures. *Angew. Chem., Int. Ed.* **2018**, *57*, 5684−5689.
(20) Kreno, L. E.; Leong, K.; Farha, O. K.; Allendorf, M.; Van Duyne, R. P.; Hupp, J. T. Metal-organic framework materials as chemical sensors. *Chem. Rev.* **2012**, *112*, 1105−1125.
(21) Engel, E. R.; Jouaiti, A.; Bezuidenhout, C. X.; Hosseini, M. W.; Barbour, L. J. Activation-Dependent Breathing in a Flexible Metal−Organic Framework and the Effects of Repeated Sorption/Desorption Cycling. *Angew. Chem., Int. Ed.* **2017**, *56*, 8874−8878.
(22) Bourrelly, S.; Llewellyn, P. L.; Serre, C.; Millange, F.; Loiseau, T.; Férey, G. Different Adsorption Behaviors of Methane and Carbon Dioxide in the Isotypic Nanoporous Metal Terephthalates MIL-53 and MIL-47. *J. Am. Chem. Soc.* **2005**, *127*, 13519−13521.
(23) Serre, C.; Mellot-Draznieks, C.; Surble, S.; Audebrand, N.; Filinchuk, Y.; Ferey, G. Role of solvent-host interactions that lead to very large swelling of hybrid frameworks. *Science* **2007**, *315*, 1828−1831.
(24) Serre, C.; Millange, F.; Thouvenot, C.; Noguès, M.; Marsolier, G.; Louër, D.; Férey, G. Very Large Breathing Effect in the First Nanoporous Chromium(III)-Based Solids: MIL-53 or $Cr^{III}(OH)\cdot\{O_2C-C_6H_4-CO_2\}\cdot\{HO_2C-C_6H_4-CO_2H\}_x\cdot H_2O_y$. *J. Am. Chem. Soc.* **2002**, *124*, 13519−13526.
(25) Mulfort, K. L.; Farha, O. K.; Malliakas, C. D.; Kanatzidis, M. G.; Hupp, J. T. An interpenetrated framework material with hysteretic CO_2 uptake. *Chem. - Eur. J.* **2010**, *16*, 276−281.
(26) Hyun, S.-m.; Lee, J. H.; Jung, G. Y.; Kim, Y. K.; Kim, T. K.; Jeoung, S.; Kwak, S. K.; Moon, D.; Moon, H. R. Exploration of Gate-Opening and Breathing Phenomena in a Tailored Flexible Metal−Organic Framework. *Inorg. Chem.* **2016**, *55*, 1920−1925.
(27) Devic, T.; Horcajada, P.; Serre, C.; Salles, F.; Maurin, G.; Moulin, B.; Heurtaux, D.; Clet, G.; Vimont, A.; Greneche, J. M.; Le Ouay, B.; Moreau, F.; Magnier, E.; Filinchuk, Y.; Marrot, J.; Lavalley, J. C.; Daturi, M.; Ferey, G. Functionalization in flexible porous solids: effects on the pore opening and the host-guest interactions. *J. Am. Chem. Soc.* **2010**, *132*, 1127−1136.
(28) Dybtsev, D. N.; Chun, H.; Kim, K. Rigid and flexible: a highly porous metal-organic framework with unusual guest-dependent dynamic behavior. *Angew. Chem., Int. Ed.* **2004**, *43*, 5033−5036.
(29) Bhatt, P. M.; Batisai, E.; Smith, V. J.; Barbour, L. J. Creation of new guest accessible space under gas pressure in a flexible MOF: multidimensional insight through combination of in situ techniques. *Chem. Commun.* **2016**, *52*, 11374−11377.
(30) Bezuidenhout, C. X.; Smith, V. J.; Bhatt, P. M.; Esterhuysen, C.; Barbour, L. J. Extreme Carbon Dioxide Sorption Hysteresis in Open-Channel Rigid Metal−Organic Frameworks. *Angew. Chem., Int. Ed.* **2015**, *54*, 2079−2083.
(31) Dietzel, P. D. C.; Johnsen, R. E.; Fjellvag, H.; Bordiga, S.; Groppo, E.; Chavan, S.; Blom, R. Adsorption properties and structure of CO_2 adsorbed on open coordination sites of metal-organic framework Ni_2(dhtp) from gas adsorption, IR spectroscopy and X-ray diffraction. *Chem. Commun.* **2008**, 5125−5127.
(32) Springuel-Huet, M.-A.; Nossov, A.; Adem, Z.; Guenneau, F.; Volkringer, C.; Loiseau, T.; Férey, G.; Gédéon, A. 129Xe NMR Study of the Framework Flexibility of the Porous Hybrid MIL-53(Al). *J. Am. Chem. Soc.* **2010**, *132*, 11599−11607.

DOI: 10.1021/acscentsci.8b00378
ACS Cent. Sci. 2018, 4, 1194−1200

(33) Llewellyn, P. L.; Maurin, G.; Devic, T.; Loera-Serna, S.; Rosenbach, N.; Serre, C.; Bourrelly, S.; Horcajada, P.; Filinchuk, Y.; Férey, G. Prediction of the Conditions for Breathing of Metal Organic Framework Materials Using a Combination of X-ray Powder Diffraction, Microcalorimetry, and Molecular Simulation. *J. Am. Chem. Soc.* **2008**, *130*, 12808−12814.
(34) Devic, T.; Salles, F.; Bourrelly, S.; Moulin, B.; Maurin, G.; Horcajada, P.; Serre, C.; Vimont, A.; Lavalley, J.-C.; Leclerc, H.; Clet, G.; Daturi, M.; Llewellyn, P. L.; Filinchuk, Y.; Férey, G. Effect of the organic functionalization of flexible MOFs on the adsorption of CO_2. *J. Mater. Chem.* **2012**, *22*, 10266−10273.
(35) Jacobs, T.; Lloyd, G. O.; Gertenbach, J.-A.; Müller-Nedebock, K. K.; Esterhuysen, C.; Barbour, L. J. In Situ X-ray Structural Studies of a Flexible Host Responding to Incremental Gas Loading. *Angew. Chem., Int. Ed.* **2012**, *51*, 4913−4916.
(36) Takamizawa, S.; Takasaki, Y.; Miyake, R. Host-guest transformational correlations for a gas inclusion co-crystal on changing gas pressure and temperature. *Chem. Commun.* **2009**, 6625−6627.
(37) Chen, L.; Mowat, J. P. S.; Fairen-Jimenez, D.; Morrison, C. A.; Thompson, S. P.; Wright, P. A.; Düren, T. Elucidating the Breathing of the Metal−Organic Framework MIL-53(Sc) with ab Initio Molecular Dynamics Simulations and in Situ X-ray Powder Diffraction Experiments. *J. Am. Chem. Soc.* **2013**, *135*, 15763−15773.
(38) Banerjee, D.; Wang, H.; Plonka, A. M.; Emge, T. J.; Parise, J. B.; Li, J. Direct Structural Identification of Gas Induced Gate-Opening Coupled with Commensurate Adsorption in a Microporous Metal-Organic Framework. *Chem. - Eur. J.* **2016**, *22*, 11816−11825.
(39) Bon, V.; Klein, N.; Senkovska, I.; Heerwig, A.; Getzschmann, J.; Wallacher, D.; Zizak, I.; Brzhezinskaya, M.; Mueller, U.; Kaskel, S. Exceptional adsorption-induced cluster and network deformation in the flexible metal-organic framework DUT-8(Ni) observed by in situ X-ray diffraction and EXAFS. *Phys. Chem. Chem. Phys.* **2015**, *17*, 17471−17479.
(40) Cui, K.-H.; Yao, S.-Y.; Li, H.-Q.; Li, Y.-T.; Zhao, H.-P.; Jiang, C.-J.; Tian, Y.-Q. Acentric and chiral four-connected metal-organic frameworks based on the racemic binaphthol-like chiral ligand of 4-(1-H(or methyl)-imidaozol-1-yl)benzoic acid. *CrystEngComm* **2011**, *13*, 3432−3437.
(41) Spek, A. Single-crystal structure validation with the program PLATON. *J. Appl. Crystallogr.* **2003**, *36*, 7−13.
(42) Lama, P.; Barbour, L. J. Distinctive Three-Step Hysteretic Sorption of Ethane with In Situ Crystallographic Visualization of the Pore Forms in a Soft Porous Crystal. *J. Am. Chem. Soc.* **2018**, *140*, 2145−2150.
(43) Sheldrick, G. M. *SAINT Data Reduction Software*, version 6.45; Bruker AXS Inc.: Madison, WI, 2003.
(44) Sheldrick, G. M. *SADABS*, version 2.05; Bruker AXS Inc.: Madison, WI, 2002.
(45) Sheldrick, G. M. A short history of SHELX. *Acta Crystallogr., Sect. A: Found. Crystallogr.* **2008**, *64*, 112−122.
(46) Barbour, L. J. X-Seed-A software tool for supramolecular crystallography. *J. Supramol. Chem.* **2001**, *1*, 189−191.
(47) Giannozzi, P.; Baroni, S.; Bonini, N.; Calandra, M.; Car, R.; Cavazzoni, C.; Ceresoli, D.; Chiarotti, G. L.; Cococcioni, M.; Dabo, I.; Dal Corso, A.; de Gironcoli, S.; Fabris, S.; Fratesi, G.; Gebauer, R.; Gerstmann, U.; Gougoussis, C.; Kokalj, A.; Lazzeri, M.; Martin-Samos, L.; Marzari, N.; Mauri, F.; Mazzarello, R.; Paolini, S.; Pasquarello, A.; Paulatto, L.; Sbraccia, C.; Scandolo, S.; Sclauzero, G.; Seitsonen, A. P.; Smogunov, A.; Umari, P.; Wentzcovitch, R. M. QUANTUM ESPRESSO: a modular and open-source software project for quantum simulations of materials. *J. Phys.: Condens. Matter* **2009**, *21*, 395502−395521.
(48) Barone, V.; Casarin, M.; Forrer, D.; Pavone, M.; Sambi, M.; Vittadini, A. Role and effective treatment of dispersive forces in materials: Polyethylene and graphite crystals as test cases. *J. Comput. Chem.* **2009**, *30*, 934−939.

DOI: 10.1021/acscentsci.8b00378
ACS Cent. Sci. 2018, 4, 1194−1200